Cell Stress and Chaperones (2021) 26:387–401
https://doi.org/10.1007/s12192-020-01184-z

ORIGINAL PAPER

# Hydrolyzed camel whey protein alleviated heat stress-induced hepatocyte damage by activated Nrf2/HO-1 signaling pathway and inhibited NF-κB/NLRP3 axis

Donghua Du[1,2] · Wenting Lv[1,2] · Rina Su[1] · Chunwei Yu[1] · Xiaoxia Jing[1] · Nuwenqimuge Bai[1] · Surong Hasi[1,3]

Received: 15 July 2020 / Revised: 16 November 2020 / Accepted: 27 November 2020 / Published online: 6 January 2021


## Abstract

Liver damage is the most severe complication of heat stress (HS). Hydrolyzed camel whey protein (CWP) possesses bioactive peptides with obviously antioxidant and anti-inflammatory activities. The current study aims to investigate whether CWP that is hydrolyzed by a simulated gastrointestinal digestion process, named S-CWP, protects BRL-3A hepatocytes from HS-induced damage via antioxidant and anti-inflammatory mechanisms. BRL-3A cells were pretreated with S-CWP before being treated at 43 °C for 1 h, and the levels of the cellular oxidative stress, inflammation, apoptosis, biomarkers for liver function, the activities of several antioxidant enzymes, and the cell viability were analyzed. The expression level of pivotal proteins in correlative signaling pathways was evaluated by western blotting. We confirmed that S-CWP alleviated HS-induced hepatocytes oxidative stress by decreased reactive oxygen species (ROS), nitric oxide (NO), 8-Hydroxy-2′-deoxyguanosine (8-OHdG), lipid peroxidation (LPO), protein carbonylation (PCO), and the activities of NADPH oxidase while enhanced superoxide dismutase (SOD), catalase (CAT), glutathione peroxidase (GSH-Px), heme oxygenase-1 (HO-1) activities, and GSH content. S-CWP suppressed HS-induced inflammatory response by reducing the phosphorylation of NF-κB p65, the expression of NLRP3, and caspase-1 and finally alleviated caspase-3-mediated apoptosis. S-CWP also alleviated HS-induced hepatocyte injury by reducing alanine aminotransferase (ALT), aspartate aminotransferase (AST), and alkaline phosphatase (ALP) levels and restoring Heat Shock Protein 70 (HSP70) expression. Furthermore, S-CWP treatment significantly enhanced the expression of NF-E2-related nuclear factor erythroid-2 (Nrf2) and HO-1. The antioxidant and anti-inflammatory effects of S-CWP were weakened by ML385, a specific Nrf2 inhibitor. Additionally, zinc protoporphyrin (ZnPP), a specific HO-1 inhibitor, significantly reversed S-CWP-induced reduction in the phosphorylation of NF-κB p65. Thus, our results revealed that S-CWP protected against HS-induced hepatocytes damage via activating the Nrf2/HO-1 signaling pathway and inhibiting NF-κB/NLRP3 axis.

**Keywords** Camel whey protein · Heat stress · Oxidative stress · Apoptosis · Hepatocyte

## Introduction

Animals subjected to continuous heat stress (HS) exhibit physiological changes such as increased core body temperature, loss of appetite, and decreased immunity, accompanied by structural and functional damage to tissues and organs (Badr et al. 2018b; Miller-Cushon et al. 2019; Nawab et al. 2018; Zaboli et al. 2019). Liver damage and failure are known as fatal complications after humans and animals suffered HS (Geng et al. 2015; Weigand et al. 2007; Hassanein et al. 1992). Although the exact molecular mechanism of HS-induced hepatocyte damage remains unclear, it reportedly involves oxidative stress and inflammation (Akbarian et al. 2016; Badr et al. 2018b; Slimen et al. 2014).

Donghua Du and Wenting Lv contributed equally to this work.

✉ Surong Hasi
surong@imau.edu.cn

[1] Key Laboratory of Clinical Diagnosis and Treatment Technology in Animal Disease, Ministry of Agriculture, College of Veterinary Medicine, Inner Mongolia Agricultural University, Hohhot 010018, China

[2] Department of Veterinary Medicine, College of Animal Science and Technology, Hebei North University, Zhangjiakou 075131, Hebei, China

[3] Inner Mongolia institute of Camel Research, Badain Jaran 075131, Inner Mongolia, China

One of the adverse effects of HS is to promote the overproduction of reactive oxygen species (ROS), which leads to the occurrence of oxidative stress (Akbarian et al. 2016; Altan et al. 2003). Then, the oxidative stress further leads to cell damage, mainly including lipid peroxidation, decarboxylation of amino acid, and DNA strand breakage (Corrochano et al. 2018). Animals and humans have evolved the antioxidant system to control the level of ROS (Akbarian et al. 2016; Slimen et al. 2014), which includes cytoprotective enzymes and antioxidants, such as superoxide dismutase (SOD), catalase (CAT), glutathione peroxidase (GSH-Px), heme oxygenase-1 (HO-1), etc. (Akbarian et al. 2016). They convert ROS to water molecules and oxygen and preserve the normal level of ROS (Andersen et al. 1997; Slimen et al. 2014; Song et al. 2018). However, excessive production of ROS can lead to oxidative stress and activate the NF-κB signaling, which in turn promotes the release of proinflammatory factors such as NOD-leucine rich repeat and pyrin containing protein 3 (NLRP3) inflammasome, leading to massive mitochondrial dysfunction, apoptosis and liver injury (Badr et al. 2018a; Guo et al. 2015; Shen et al. 2014). Moreover, studies have further confirmed that NLRP3 is essential in mediating HS-induced liver injury (Geng et al. 2015). NF-E2-related nuclear factor erythroid-2 (Nrf2) plays an important role in regulating cytoprotective enzyme expression and resisting oxidative stress. Studies have confirmed that the Nrf2 can regulate the inflammatory cascade by inhibiting NF-κB signaling and decreasing the level of proinflammatory factors (Wardyn et al. 2015). Therefore, regulating the NF-κB/NLRP3 axis through the Nrf2 signaling pathway may be a potential treatment for HS-induce hepatocyte damage.

Camel whey protein (CWP) is a powerful natural antioxidant because it inhibits ROS production, alleviates oxidative stress and inflammation, and increases GSH levels (Badr et al. 2017a). CWP is similar in composition to bovine whey protein but lacks β-lactoglobulin (β-LG). LG is the major cause of milk allergies in children (Badr et al. 2017a, b, 2018b; Elagamy 2000; Ramadan et al. 2018). In addition, CWP or camel milk (CM) has higher antioxidant activities than WPs or milk from bovine and other animals (Badr et al. 2017a; Elagamy 2000; Mihic et al. 2016). In terms of anti-HS, CWP inhibited HS-induced oxidative stress, inflammation, and apoptosis of mice lymphocytes via the PI3K/AKT, NF-κB signaling pathways (Badr et al. 2018b), and attenuated HS-induced testis damage through the YAP/Nrf2 pathway (Badr et al. 2018a) and also restored GHS levels in the liver (Abdel-Aziem et al., 2011). The antioxidant activity of WP may be attributed to the production of bioactive peptides in the digestive tract (Udenigwe and Aluko 2012; O'Keeffe and FitzGerald 2014). Furthermore, a study has shown that peptides produced by enzymatic hydrolysis of CWP exhibited a stronger ability to reduce the chemical radical DPPH than their undigested proteins (Ibrahim et al. 2018). However, its ability to alleviate HS-induced hepatocyte injury has not been demonstrated yet. Therefore, we investigated the anti-HS effect of simulated gastrointestinal digestion of CWP (S-CWP) in hepatocytes, and the emphasis is placed on its regulatory effect on Nrf2 signaling and NF-κB/NLRP3 axis.

## Materials and methods

### Pretreatment of camel milk

The fresh Bactrian camel milk (CM) was collected aseptically from at least 20 healthy camels of the local farm in Alashan, Inner Mongolia, China. The samples were blended to obtain a homogenous sample and then immediately kept in cold storage at 4 °C and transported to the laboratory within 2 h followed by the degreasing and pasteurization process. Briefly, raw milk was spun at 1400×*g* and 4 °C for 30 min, and then the creamy layer was removed; thereafter, defatted CM was heated at 80 °C for 20 min and cooled to 43–45 °C immediately (Hamed et al. 2018; Ramadan et al. 2018). Samples were freeze-dried and kept at − 80 °C until use.

### Preparation of camel whey protein

CWP was prepared by means of referent papers (Badr et al. 2017b, 2018b). Briefly, the pH of the skim CM was adjusted to 4.3 with 1 M HCl and then centrifuged at 11000×*g* and 4 °C for 10 min. The supernatant after centrifugation was collected, which was the sample of CWP after precipitation of the casein. CWPs were precipitated by using ammonium sulfate and then dialyzed for 48 h by using a dialysis bag with a molecular weight cut-off of 6000–8000 kDa, in which the ratio of CWP to distilled water was 1:20. The dialysate was freeze-dried and kept at − 80 °C until use.

### Simulated gastrointestinal digestion of CWP (S-CWP)

The processes of simulated gastrointestinal digestion (SGID) were performed based on the pertinent reference (Power-Grant et al. 2015). Freeze-dried CWP samples were diluted with sterilized deionized water to a final concentration of 2.0% (w/w) and adjusted the pH to 2.0 with 1 M HCl. After being incubated for 30 min at 37 °C, Pepsin (Sigma, St Louis, MO, USA; Cat. No.: P7000) was then added (the ratio of enzyme to the substrate is 1:40) and incubated for another 90 min. Then, the pH of the reaction systems was adjusted to 7.5 after heat is inactivated at 90 °C for 20 min. After that, Corolase PP (CorPP; Sigma, St Louis, MO, USA; Cat. No.: T4799) was added at a ratio of enzyme to the substrate is 1:100 (w/w) and incubated at 37 °C for another 150 min and sequenced by heat inactivation at 90 °C for 20 min. The

degree of hydrolysis (DH) is defined as the percentage of total peptide bonds that are hydrolyzed in the protein, and the o-phthaldialdehyde (OPA) assay was used to detect it as described in the literature (Nielsen et al. 2001). The hydrolysate was centrifuged at 5000×*g* at 4 °C for 30 min to remove the insoluble substrate fragments. The CWP after SGID process was named S-CWP, freeze-dried, and kept at − 80 °C until use.

## Reducing SDS-PAGE of S-CWP

The degree of hydrolysis (DH) of CWP was further analyzed on reducing SDS-PAGE according to referent papers (Ibrahim et al. 2018; Wang et al. 2020). In brief, S-CWP (0.4 mg) was mixed with 1 ml of reducing sample buffer and then heated at 95 °C for 5 min. Samples (10 μl) were loaded into 12% acrylamide gels for electrophoresis. The gel was run at 80 V for 30 min and then for 60 min at 120 V. The gel was fixed for 12 h at room temperature. Protein bands were visualized with Feto Protein Staining Buffer (2 h at room temperature), a Coomassie bright blue R250 fast staining solution (Solarbio Science & Technology, Beijing, China; Cat. No.: G4540). After staining, the gel was stored in water and taken out to take pictures.

## Cell culture and treatment

Normal *Rattus norvegicus* hepatocytes (BRL-3A) were purchased from the Procell Life Science and Technology Co., Ltd. (Wuhan, China; Cat. No.: CL-0036). Cells were cultured in DMEM (Gibco, NY, USA) supplemented with 10% (v/v) FBS (Gibco, NY, USA), streptomycin (100 μg/ml), and penicillin (100 U/ml) and maintained at 37 °C in a humidified $CO_2$ (5%, v/v) incubator. A HS-induced cell injury model was established using a stable rat hepatic cell line BRL-3A as described in the references (Geng et al. 2015). In brief, when BRL-3A cells reached a confluence of 70–80%, they were pretreated with S-CWP (10, 30, or 50 μg/ml) for 12 h, followed by HS treatment for 1 h at 43 °C. After 9-h recovery at 37 °C, cells and the supernatants were harvested. The above supplemental dose of S-CWP has been confirmed to be non-cytotoxic by MTT assay in previous pre-experiments. In other separate experiments, cells were pretreated with an Nrf2 inhibitor (ML385, 10 μM; MCE, NJ, USA; Cat. No.: HY-100523), a HO-1 inhibitor (ZnPP, 10 μM; MCE; Cat. No.: HY-101193), or an NF-κB inhibitor (Berbamine dihydrochloride, 10 μM; MCE; Cat. No.: HY-N0714A) for 1 h prior to S-CWP treatment.

## Detection of cell viability

The MTT assay was performed with the instruction of MTT Cell Proliferation and Cytotoxicity Detection Kit (Keygenbio Biotechnology, Nanjing, China; Cat. No.: KGA312). In brief, the cells were seeded at a density of 3000 cells (100 μL) per well in 96-well plates. After the cells suffered HS treatment, 50 μl of 1 × MTT solution was added to each well and incubated at 37 °C for another 4 h, and then the medium was replaced with 150 μl DMSO and vortexes for 10 min. At the wavelength of 490 nm, the absorbance of each well was detected with a microplate reader (Synergy H4, BioTek, USA).

## Extraction of total cellular protein

The cells were seeded at a density of $1 \times 10^6$ cells (2 ml) per well in 6-well plates. After being treated as previously described, the cells were washed three times with ice-cold PBS and then lysed on ice in 100 μl cell buffer for Western and IP (Beyotime Biotechnology, Shanghai, China; Cat. No.: P0013) containing protease inhibitor (5 mg/ml; Thermo Fisher Scientific, Shanghai, China; Cat. No.: A32963) and PMSF (0.1 mM) for 30 min. Then, cells were collected by cell scraper and centrifuged at 14000×*g* for 5 min at 4 °C to obtain the supernatant. The protein concentrations were determined by using the Pierce BCA Protein Assay Kit (Thermo Fisher Scientific, Shanghai, China; Cat. No.: 23225). Cell culture supernatant was spun at 2000×*g* for 20 min, and then the supernatant was collected. Nuclear protein extraction was performed according to the kit instructions (Sangon Biotech, Shanghai, China; Cat. No.:C500009).

## Detection of markers of oxidative stress

Intracellular ROS levels were detected by Reactive Oxygen Species (ROS) Assay Kit (Beyotime Biotechnology, Shanghai, China; Cat. No.: S0033), which is an assay by using 2′,7′-dichlorodihydrofluorescein diacetate (DCFH-DA). Briefly, BRL-3A cells were seeded in 6-well plates at a density of $1 \times 10^6$ cells (2 ml) and incubated for 24 h before being pretreated with S-CWP for 12 h. Then, DCFH-DA diluted with the serum-free medium was added to the wells at a final concentration of 10 μM and incubated at 37 °C for 20 min followed by treated with heat stress (43 °C) for another 1 h. The cells were washed three times with serum-free cell culture medium to remove DCFH-DA that did not enter the cells. Cells loaded with probes were visualized by using a fluorescence microscope (Olympus, IX71, Tokyo, Japan). The excitation wavelength of 488 nm and the emission wavelength of 525 nm were used to detect the fluorescence intensity in the cells by using a fluorescence microplate reader (Synergy H4, BioTek, USA). Nitric oxide (NO) in the cell culture supernatant was measured by using Griess reagent with NO detection kit (Beyotime Biotechnology, Shanghai, China; Cat. No.: S0021). Lipid peroxidation (LPO), 8-Hydroxy-2′-deoxyguanosine (8-OH-dG), a marker of DNA damage, and protein carbonylation (PCO), a marker of protein damage,

were detected by lipid peroxidation assay kit (Cat. No.: A106-1), 8-hydroxydeoxyguanosine Assay Kit (Cat. No.: H165), and Protein Carbonyl (PCO) Colorimetric Assay Kit (Cat. No.: A087), respectively (Nanjing Jiancheng Bioengineering Institute, Nanjing, China).

## Detection of antioxidants and cytoprotective enzymes

The activities of the intracellular NADPH oxidase, SOD, CAT, GSH-Px, and the ratio of reduced glutathione (GSH)/oxidized glutathione disulfide (GSSG) were detected by using commercial kits according to the instruction manuals of Nanjing Jiancheng Bioengineering Institute (Nanjing, China). Total HO-1 activity was detected to follow the assay of previous research (Abraham et al. 1985). In brief, cell lysate was mixed with 2 mM glucose-6-phosphate, 0.2 U glucose-6-phosphate dehydrogenase, 20 μM hemin, and 0.8 mM NADPH (Sigma, St Louis, MO, USA; Cat. No.: 481974) in a total volume of 1.2 ml. After being incubated for 1 h at 37 °C, the absorbance was recorded at 464 nm.

## Determination of NLRP3, caspases, and biomarkers for liver function

NACHT, LRR, and PYD domain-containing protein 3(NLRP3) was detected by using ELISA kit (HCUSABIO, Wuhan, China; Cat. No.: CSB-EL015871MO). Caspase-1 in cells was measured by using Rat Caspase-1(CASP1) ELISA kit (HCUSABIO, Wuhan, China; Cat. No.: CSB-EL004543RA). The activity of caspase 3 in cells was determined by using the Caspase 3 Activity Assay Kit (Beyotime Biotechnology, Shanghai, China; Cat. No.: C1116), according to the manufacturer's protocols. The relative caspase-3 activity is described as the ratio to that of the control group. The levels of alanine aminotransferase (ALT), aspartate aminotransferase (AST), and alkaline phosphatase (ALP) in the cell culture supernatant were measured by using commercial kits (Nanjing Jiancheng Bioengineering Institute, Nanjing, China).

## Morphological detection of apoptotic cells

Apoptosis was evaluated by Annexin V-FITC Apoptosis Detection Kit (Beyotime Biotechnology, Shanghai, China; Cat. No.: C1062L), which is an assay by using Annexin V-FITC labeling phosphatidyl serine (PS) present on the cell membrane surface during apoptosis and propidium iodide (PI) labeling DNA. Briefly, the cells were seeded at a density of $5 \times 10^4$ cells per well in 24-well plates. Following treatment as previously mentioned, 24-well plates were spun at 1000×*g* for 5 min, and then the cell culture medium was removed, and the cells washed once with PBS. Then, 24-well plates were spun at 1000×*g* for 5 min again. After that, Annexin V-FITC binding fluid (195 μL), Annexin V-FITC (5 μL), and PI (10 μL) were added into each well in sequence. After gently mixing, cells were incubated in dark for 10–20 min at room temperature (20–25 °C) and then visualized by using a fluorescence microscope (Zeiss, AX10, Jena, Germany).

## Real-time PCR

Total RNA was extracted by using Trizol reagent. The cDNA was generated by using HiScript Q RT SuperMix for qPCR (Vazyme, Nanjing, China; Cat. No.: R122-01). The qPCR was performed by using Cham Q SYBR qPCR Master Mix (Vazyme, Nanjing, China; Cat. No.: Q341-02/03) on an ABI Quantstudio 7. The relative mRNA expression was calculated by using $2^{-\triangle\triangle Ct}$ method. The primer sequences are presented in Table 1.

## Western blotting analysis

Cells were lysed in 100 μl cell buffer for western and IP as mentioned above. The protein concentrations were determined by using a BCA protein assay kit. Then, equal amounts of total cellular protein (20 μg) were mixed with loading buffer and separated by 10% SDS-PAGE. The gel was run at 120 V for 80 min before being transferred onto a polyvinylidene fluoride (PVDF) membrane (Amersham, GE Healthcare, Velizy-Villacoublay, France) at 80 V for 45 min. After the PFDF membranes were blocked with QuickBlock™ Blocking Buffer (Beyotime, Shanghai, China; Cat. No.: P0252) for 1 h, they were incubated with rabbit anti-HSP70 (1:1000; CST, Danvers, USA; Cat. No.: 3033), rabbit anti-Nrf2 (1:2000; Abcam, Camb, UK; Cat. No.: ab31163), rabbit anti-HO-1 (1:1000; GeneTex, Inc., USA; Cat. No.: GTX30748), rabbit anti-NF-κB p65(1:1000; CST, Danvers, USA; Cat. No.: 4764), rabbit anti-NF-κB p65 (phospho S536) (1:1000; CST, Danvers, USA; Cat. No.: 3033), and rabbit anti-β-actin antibody (1:10000; Abcam, Camb, UK; Cat. No.: ab8227) overnight at 4 °C. Then, the membranes were washed three times with TBST and incubated with Goat anti-Rabbit IgG (H + L)-HRP (Tianjin Sungene Biotech, Tianjin, China; Cat. No.: LK2001) at a dilution of 1:5000 for 45 min at room temperature. The membranes were washed the same as before and visualized by using Super ECL Plus (US Everbright Inc., Suzhou, Jiangsu, China; Cat. No.: S6009). Then, the images were detected by using the Odyssey infrared imaging system (LI-COR Biosciences) and analyzed by the Image-Pro Plus 6.0 software (Media Cybernetics, Maryland, USA). The protein bands' density was normalized based on the β-actin in the same samples.

**Table 1** The primer sequences for real-time PCR

| | | |
|---|---|---|
| NF-κB p65 (NCBI Gene ID: 309165) | Forward | 5′-GGGATGGCTTCTATGAGGCTGAAC-3′ |
| | Reverse | 5′-CTTGCTCCAGGTCTCGCTTCTTC-3′ |
| NLRP3 (NCBI Gene ID: 287362) | Forward | 5′-GAGCTGGACCTCAGTGACAATGC-3′ |
| | Reverse | 5′-ACCAATGCGAGATCCTGACAACAC-3′ |
| Caspase-1 (NCBI Gene ID: 25166) | Forward | 5′-AAACACCCACTCGTACACGTCTTG-3′ |
| | Reverse | 5′-AGGTCAACATCAGCTCCGACTCTC-3′ |
| Nrf2 (NCBI Gene ID: 83619) | Forward | 5′-GCCTTCCTCTGCTGCCATTAGTC-3′ |
| | Reverse | 5′-TCATTGAACTCCACCGTGCCTTC-3′ |
| HO-1 (NCBI Gene ID: 24451) | Forward | 5′-CAGACAGAGTTTCTTCGCCAGAGG-3′ |
| | Reverse | 5′-TGTGAGGACCCATCGCAGGAG-3′ |
| β-actin | Sangon Biotech, Shanghai, China; Cat. No.: B661202 | |

### Statistical analyses

The data was analyzed by using SPSS 25.0 software and presented as means ± SEM. Samples lacking normality were analyzed using Wilcoxon Rank Sum Test. Samples that met normality were compared by the Wilcoxon Rank Sum Test with Tukey post-test when variances were equal. In the case of unequal variance, the Kruskal-Wallis Test was used. The results were considered significant at $p < 0.05$. Adobe Illustrator CC 2019 and GraphPad Prism 8.0 were used to visualize the results.

## Results

### Simulated gastrointestinal digestion of CWP

In the present research, hydrolysates of CWP (S-CWP) by using a process of simulated gastrointestinal digestion (SGID) had DH values of 32.41%. S-CWP was analyzed on reducing SDS-PAGE (Fig. 1). CWP had been almost completely hydrolyzed into peptides with small molecular masses that less than 10 kDa. It also showed that CWP lacks β-LG.

### S-CWP alleviated HS-induced oxidative stress and enhanced cell viability

The potential beneficial effects of S-CWP on HS-induced oxidative stress in BRL-3A cells were evaluated by the production of intracellular ROS, LPO, 8-OHdG, PCO, and the NO content in the cell culture supernatant. Thiobarbituric acid reactive species (TBARS) were detected as an LPO marker. Cell viability can be reduced by HS or oxidative stress, so we also evaluated the effect of S-CWP on it. The results showed that HS induced a significant increase of intracellular ROS (Fig. 2a and b), LPO (Fig. 2c), 8-OHdG (Fig. 2d), PCO (Fig. 2e), and NO (Fig. 2f) levels, while significant decreased the cell viability (Fig. 2g). Interestingly, cells received S-CWP before HS treatment exhibited significantly lower levels of LPO, 8-OHdG, and PCO in a dose-dependent manner. Moreover, we found a return to normal levels of ROS and NO in cells pretreated with 50 μg/ml S-CWP. More importantly, S-CWP enhanced HS-induced reduction of cell viability in a dose-dependent manner. These data indicated that S-CWP has a noticeable alleviation on the HS-induced oxidative stress of BRL-3A cells.

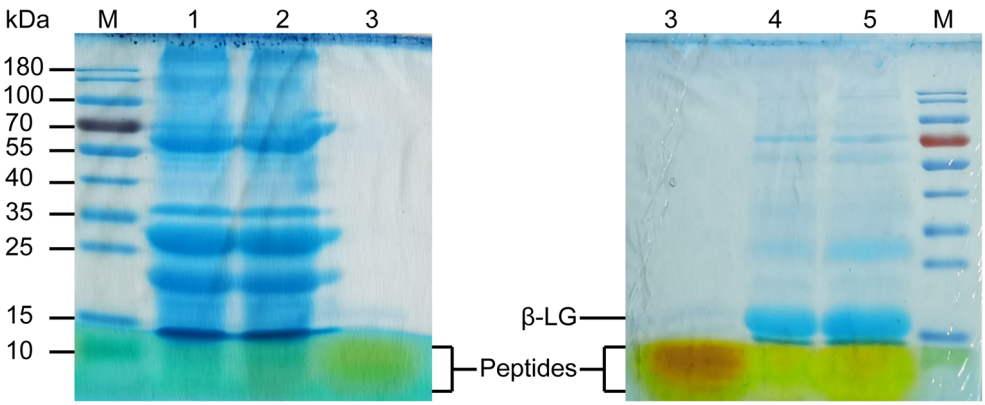


**Fig. 1** Electrophoretic patterns of CWP before and after SGID on 12% reducing SDS-PAGE. M: Prestained protein ladder (Thermo Fisher Scientific, Shanghai, China; Cat. No.: 26617). 1 & 2: Unhydrolyzed CWP. 3: S-CWP. 4 & 5: Unhydrolyzed milk whey protein

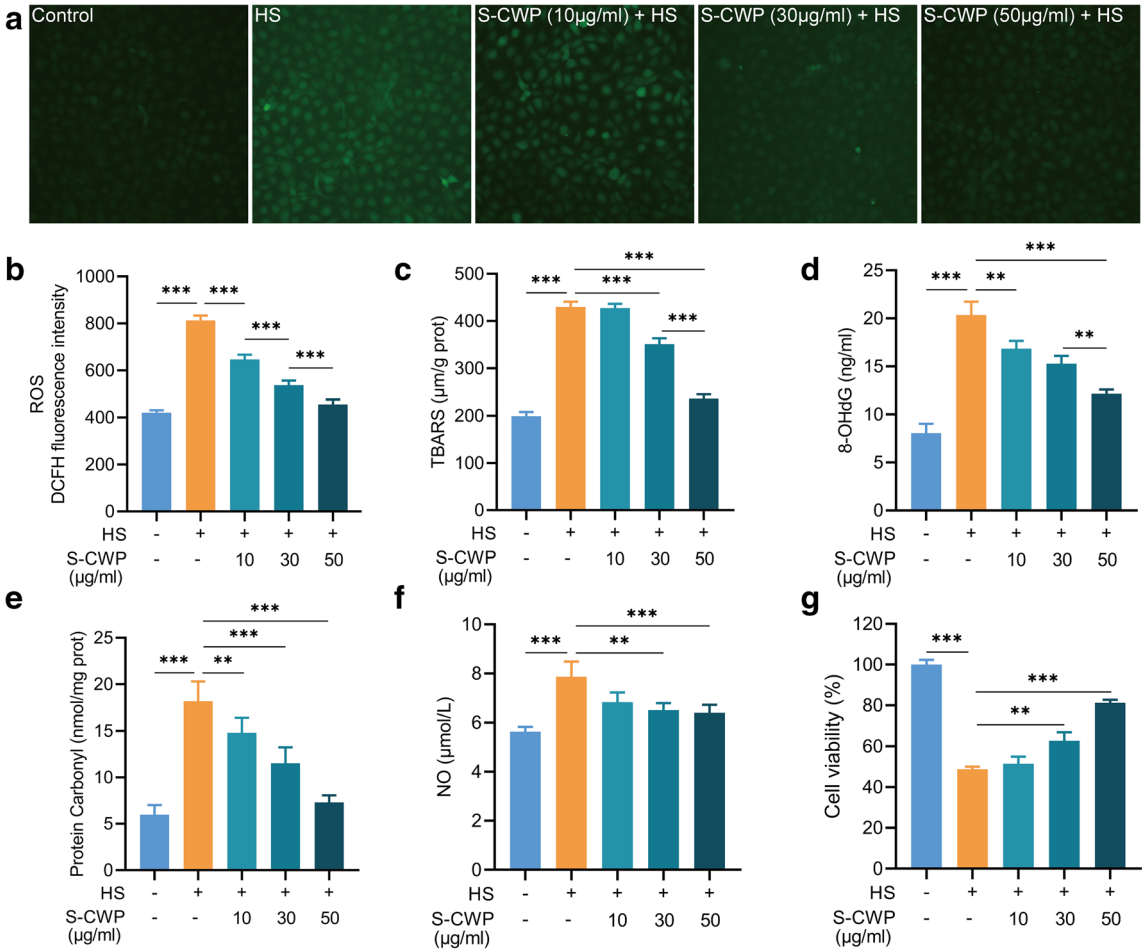


**Fig. 2** S-CWP alleviated oxidative stress in HS-treated BRL-3A cells. Cells were pretreated with 10, 30, and 50 μg/ml S-CWP before being exposed to HS. The levels of ROS were detected by using a fluorescence probe (DCFH-DA). The fluorescence was visualized by fluorescence microscope (× 100) (**a**). S-CWP reduced levels of ROS (**b**), TBARS (**c**), 8-OHdG (**d**), PCO (**e**), NO (**f**), and enhanced cell viability (**g**). Data are presented as the mean of three determinations ± SEM. $*p < 0.05$, $**p < 0.01$, and $***p < 0.001$

## S-CWP increased content of antioxidants in HS BRL-3A cells

HS promotes the generation of ROS through provoking NADPH depletion (Slimen et al. 2014). We detected the NADPH oxidase activity and the ability of antioxidant defenses in BRL-3A cells. To inhibit ROS generation and subsequent oxidative damage induced by HS, S-CWP boosted hepatocellular antioxidant defenses. NADPH oxidase activity increased significantly in HS-treated cells compared with that in normal control cells (Fig. 3a). However, this increase was effectively suppressed by pretreatment with S-CWP in a dose-dependent manner. Similarly, HS diminished activities of SOD (Fig. 3b), CAT (Fig. 3c), GSH-Px (Fig. 3d), and the ratio of GSH/GSSG (Fig. 3e). In contrast, cells received 10, 30, or 50 μg/ml S-CWP before HS exhibited noticeable promotion of hepatocellular antioxidants. And, more remarkably, HO-1 activity was significantly enhanced (Fig. 3f) compared with control cells, indicating that it may play a key role in S-CWP anti-HS-induced oxidative stress.

The above results showed that 50 μg/ml S-CWP had the best antioxidant effect and significantly increased cell viability, so this dose was used in subsequent tests.

## S-CWP alleviated inflammatory response induced by HS via NF-κB/NLRP3 axis

HS-induced liver injury is a final consequence of the inflammatory response (Geng et al. 2015). Thus, we measured the production of the NLRP3 inflammasome, a crucial inflammatory signaling factor, including its upstream signaling molecule NF-κB. Meanwhile, to determine the regulatory effect of the NF-κB signaling pathway on the inflammatory response, berbamine dihydrochloride, an inhibitor of this pathway, was used. Bapamine hydrochloride is an effective NF-κB inhibitor, which can prevent its transport into the nucleus and reduce the expression of downstream cytokines. We found that the phosphorylation of NF-κB p65 increased after cells were treated by HS (Fig. 4a). NLRP3 (Fig. 4b) and caspase-1 (Fig. 4c), which make up the NLRP3 inflammasomes,

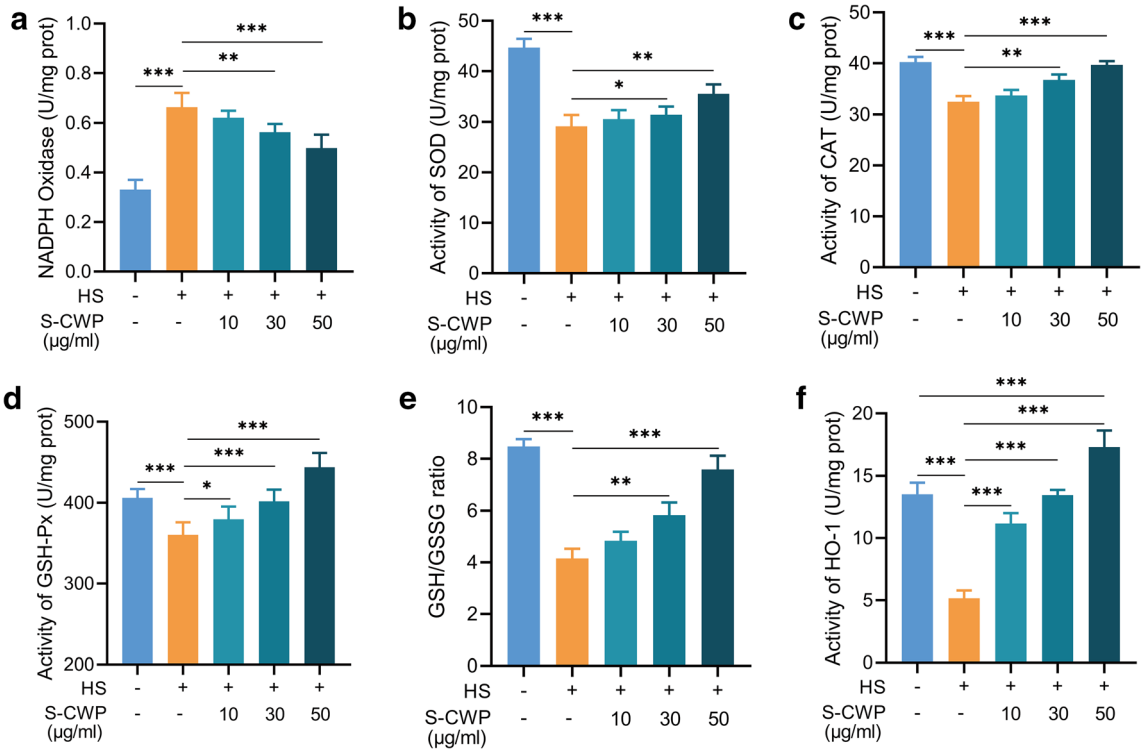


**Fig. 3** S-CWP suppressed HS-induced destruction of antioxidants in BRL-3A cells. S-CWP suppressed the activity of NADPH oxidase (Fig. 2a), increased the activity of SOD (Fig. 2b), CAT (Fig. 2c), GSH-Px (Fig. 2d), and the ratio of GSH/GSSG (Fig. 2e). Of note, the active of HO-1 was significantly increased by 50 μg/ml S-CWP compared with control cells (Fig. 2f). Data are presented as the mean of three determinations ± SEM. $*p < 0.05$, $**p < 0.01$, and $***p < 0.001$

exhibited the same trends. The expression levels of NF-κB p65, NLRP3, and caspase-1 mRNA also showed the same trend (Fig. 4d). Of note, the expression of NLRP3 and caspase-1 significantly decreased by berbamine dihydrochloride, indicating that NF-κB signaling played an important role in HS-mediated inflammatory response. Similarly, the phosphorylation of NF-κB p65 is significantly inhibited by S-CWP and the expression of NLRP3 and caspase-1 in BRL-3A cells. Therefore, our data suggested that S-CWP alleviated inflammatory response induced by HS via the NF-κB/NLRP3 axis.

## S-CWP protected liver cells from HS damage

HS-induced oxidative and inflammatory response can lead to apoptosis and subsequently liver dysfunction. We determined the effect of S-CWP on HS-induced apoptosis and levels of biomarkers for liver function. The results showed that S-CWP suppressed HS-induced increased activity of caspase-3, a critical executioner of apoptosis (Fig. 5a). In addition, treatment with HS resulted in the remarkable increase in ALT (Fig. 5b), AST (Fig. 5c), and ALP (Fig. 5d) levels in BRL-3A cells compared to that of control cells. The increased levels of these biomarkers suggested that the cells had been damaged. It has been confirmed that overexpressed HSP70 can promote the secretion of proinflammatory cytokines through the NF-κB signaling pathway, which in turn mediates cell damage (Asea et al. 2002). Therefore, we also examined the effect of S-CWP on HSP70 expression in HS cells. The data showed that HSP70 expression was significantly increased in the HS group compared with the control group, while it was significantly restored in cells pretreated with S-CWP and berbamine dihydrochloride. Thus, S-CWP and berbamine dihydrochloride both alleviated HS-induced hepatocyte damage by reversing these biomarkers, as well as caspase-3 and HSP70. Therefore, we further demonstrated that S-CWP alleviated HS-induced hepatocyte injury by inhibiting the NF-κB signaling pathway.

## S-CWP alleviated HS-induced morphological changes of BRL-3A cells

As can be seen, in the early stage of apoptosis, cells bound to Annexin V-FITC (green fluorescence) but excluded PI (red fluorescence), while necrotic and late apoptotic cells bound to both Annexin V-FITC and PI (Fig. 6). HS led to morphological changes of cells. After HS treatment, cells tended to get round in shape, small in size, and increased in the numbers of apoptosis cells. Conversely, BRL-3A cells pretreated with 50 μg/ml S-CWP or 10 μM berbamine dihydrochloride alleviated HS-induced morphological changes. These data further

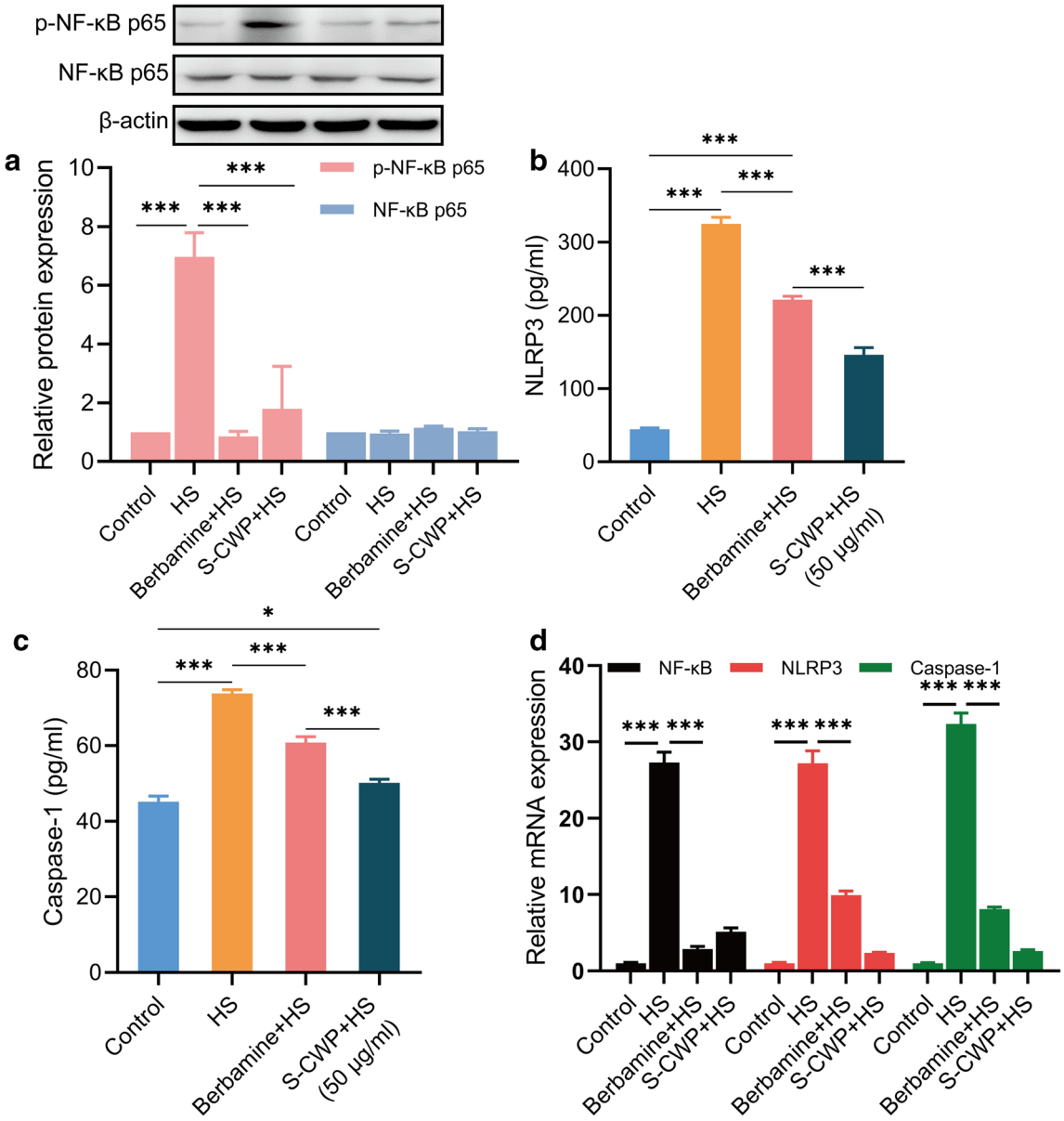


**Fig. 4** S-CWP alleviated inflammatory response induced by HS in BRL-3A cells through NF-κB/NLRP3 axis. The cells were pretreated with 10 μM berbamine dihydrochloride or 50 μg/ml S-CWP before being treated with HS. Cells were lysed and immunoblotted with NF-κB p65 and p-NF-κB p65 antibodies. The phosphorylation of NF-κB p65 is normalized based on the density of β-actin in the same samples. NLRP3 in the cell culture supernatant was detected by ELISA assay. Intracellular caspase-1 was measured by ELISA assay. Berbamine dihydrochloride is an inhibitor of NF-κB signaling. The phosphorylation of NF-κB p65 is significantly inhibited by S-CWP (**a**), as well as the expression of NLRP3 (**b**) and caspase-1 (**c**) in BRL-3A cells. The expression levels of NF-κB p65, NLRP3, and caspase-1 mRNA also showed the same trend (Fig. 4d). Data are presented as the mean of at least three determinations ± SEM. $*p < 0.05$, $**p < 0.01$, and $***p < 0.001$

confirmed the anti-HS-induced hepatocyte apoptosis effect of S-CWP via the NF-κB signaling pathway.

## S-CWP alleviated HS-induced oxidative stress and inflammatory response via the Nrf2 signaling pathway in BRL-3A cells

To investigate the effect of S-CWP on Nrf2 signaling and given the double role of HO-1 in cellular oxidative stress and inflammation, both expressions of them were measured. In this study, Nrf2 specific inhibitor ML385 was used to analyze the effect of Nrf2 signaling pathway on HS-induced inflammation. The results revealed that HS reduced Nrf2 expression in the nucleus compared with that in the control group (Fig. 7a and d). Meanwhile, the protein expression of HO-1, the downstream target of Nrf2, decreased correspondingly (Fig. 7b and d), and its activity significantly decreased by HS (Fig. 7c). Interestingly, Nrf2 and HO-1 protein

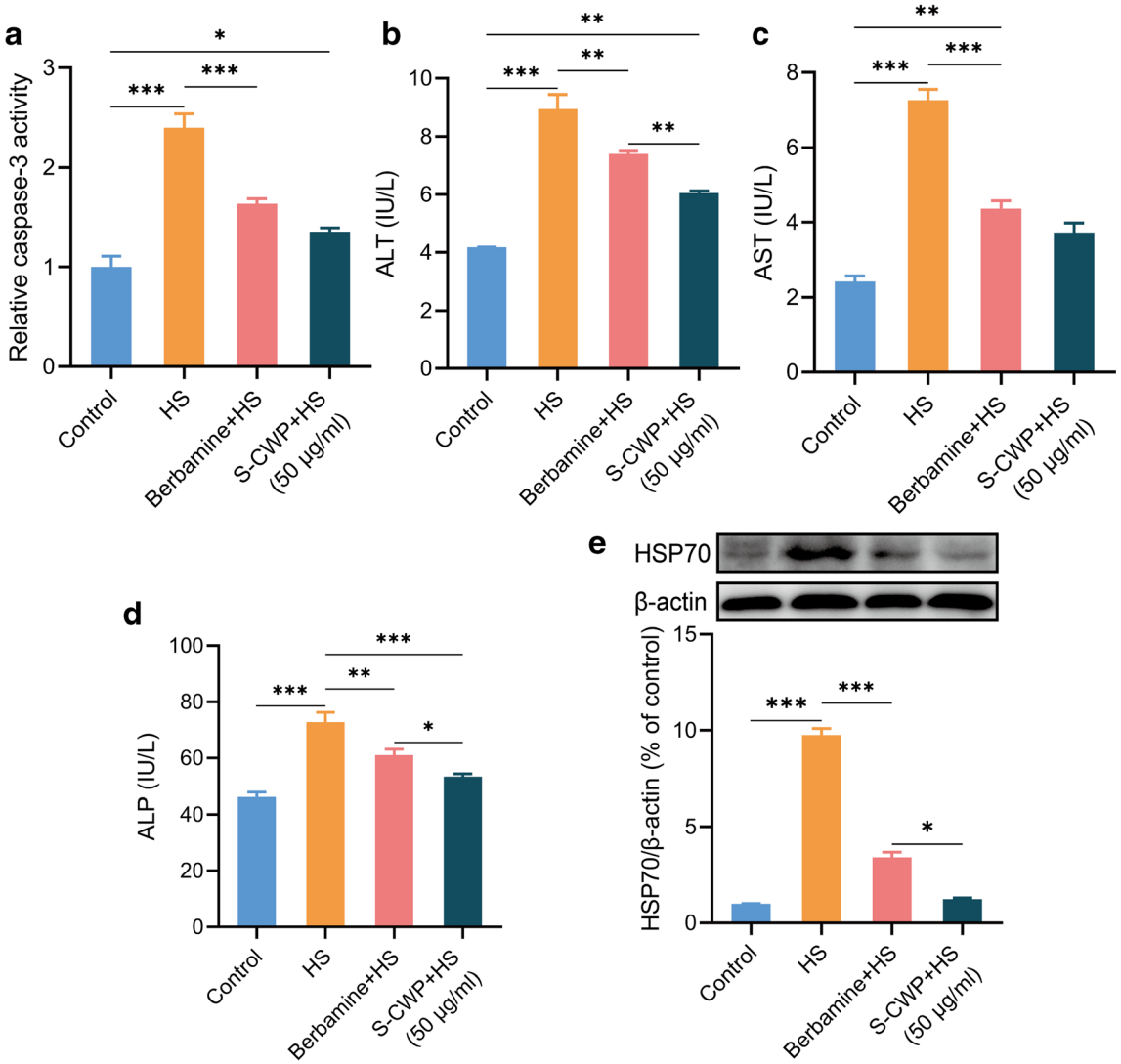


**Fig. 5** S-CWP alleviated HS-induced apoptosis and down-regulated the content of biomarkers for liver function. The cells were pretreated with 10 μM berbamine dihydrochloride or 50 μg/ml S-CWP before being treated with HS. S-CWP reduced caspase-3 activity (**a**), ALT (**b**), AST (**c**), and ALP (**d**) in BRL-3A cells. Meanwhile, S-CWP also decreased HSP70 expression (**e**). Data are presented as the mean of at least three determinations ± SEM. *$p < 0.05$, **$p < 0.01$, and ***$p < 0.001$

expression were both significantly increased in cells pretreated with 50 μg/ml S-CWP before HS treatment. In addition, S-CWP decreased intracellular ROS level (Fig. 7e), NF-κB phosphorylation level (Fig. 7f), and NLRP3 content (Fig. 7g). However, ML385 inhibited the enhancement of S-CWP on Nrf2 and HO-1, as well as the reduction on ROS, NF-κB, and NLRP3. In addition, the positive effect of S-CWP on HS-induced apoptosis was reversed by ML385 (Fig. 7i). The expression levels of Nrf2, HO-1, NF-κB, and NLRP3 mRNA also showed the same tendency as the protein expression levels (Fig. 7h). These results suggested that activation of Nrf2 is essential to protect hepatocytes from HS-induced oxidative stress and inflammatory response-mediated apoptosis. Our data also showed that S-CWP inhibited the NF-κB signaling pathway by activating the Nrf2 signaling pathway and alleviated the HS-induced oxidative stress, inflammatory response, and apoptosis in BRL-3A cells.

## S-CWP protected against HS-induced inflammatory response via upregulated HO-1 protein expression in BRL-3A cells

To investigate the anti-inflammatory effects of the Nrf2/HO-1 axis, a specific inhibitor of HO-1, zinc protoporphyrin (ZnPP), was used in the present study. Results showed that the phosphorylation of NF-κB p65, which had been inhibited by S-CWP, increased again when cells were treated with ZnPP compared to the control group (Fig. 7j). The results suggested that HO-1 was involved in the alleviative effect of S-CWP on

HS-induced increased phosphorylation of NF-κB and subsequent inflammatory response.

## Discussion

Heat stress (HS) has become one of the major environmental stressors of global warming, seriously harming the health of animals and human beings. Liver injury is the most fatal and common pathological change in almost all cases of HS (Geng et al. 2015; Weigand et al. 2007; Hassanein et al. 1992). The mechanism of HS-induced liver injury involves oxidative stress and inflammatory response (Akbarian et al. 2016; Badr et al. 2018a, b; Ramadan et al. 2018; Slimen et al. 2014). Despite the increasing understanding of HS-induced liver injury, there is no safe and effective pharmacotherapy to intervene in this severe complication. Therefore, new therapies to hamper HS-induced liver injury are in demand urgently. Milk proteins have attracted increasing attention because they are usually precursors to various bioactive peptides released during gastrointestinal digestion. Camel whey protein (CWP) is considered a powerful natural antioxidant and has been reported to exhibit greater biological activities than bovine and other whey proteins (WPs), including anti-HS, antioxidant, and anti-inflammatory activities (Chen et al. 2014; Salami et al. 2010). Previous researches have shown that the biologically active peptides (BAPs) produced by CWP

**Fig. 7** Effects of S-CWP on Nrf2/HO-1 and NF-κB signaling pathway in BRL-3A cells. Cells were pretreated with 10 μM ML385 for 1 h and then treated with 50 μg/ml S-CWP for 12 h. The protein expression of Nrf2 (**a** and **d**), HO-1 (**b** and **d**), the activity of HO-1 (**c**), the level of ROS (**e**), the expression of p-NF-κB (**f**), NLRP3 (**g**), and apoptosis (**i**) were determined. The expression levels of Nrf2, HO-1, NF-κB, and NLRP3 mRNA (**h**). Then, the cells were pretreated with 10 μM ZnPP for 1 h before being treated with S-CWP (50 μg/ml), followed by HS treatment. The phosphorylation of NF-κB p65 was determined by western blotting analysis (**j**). Data are presented as the mean of three determinations ± SEM. $*p < 0.05$, $**p < 0.01$, and $***p < 0.001$

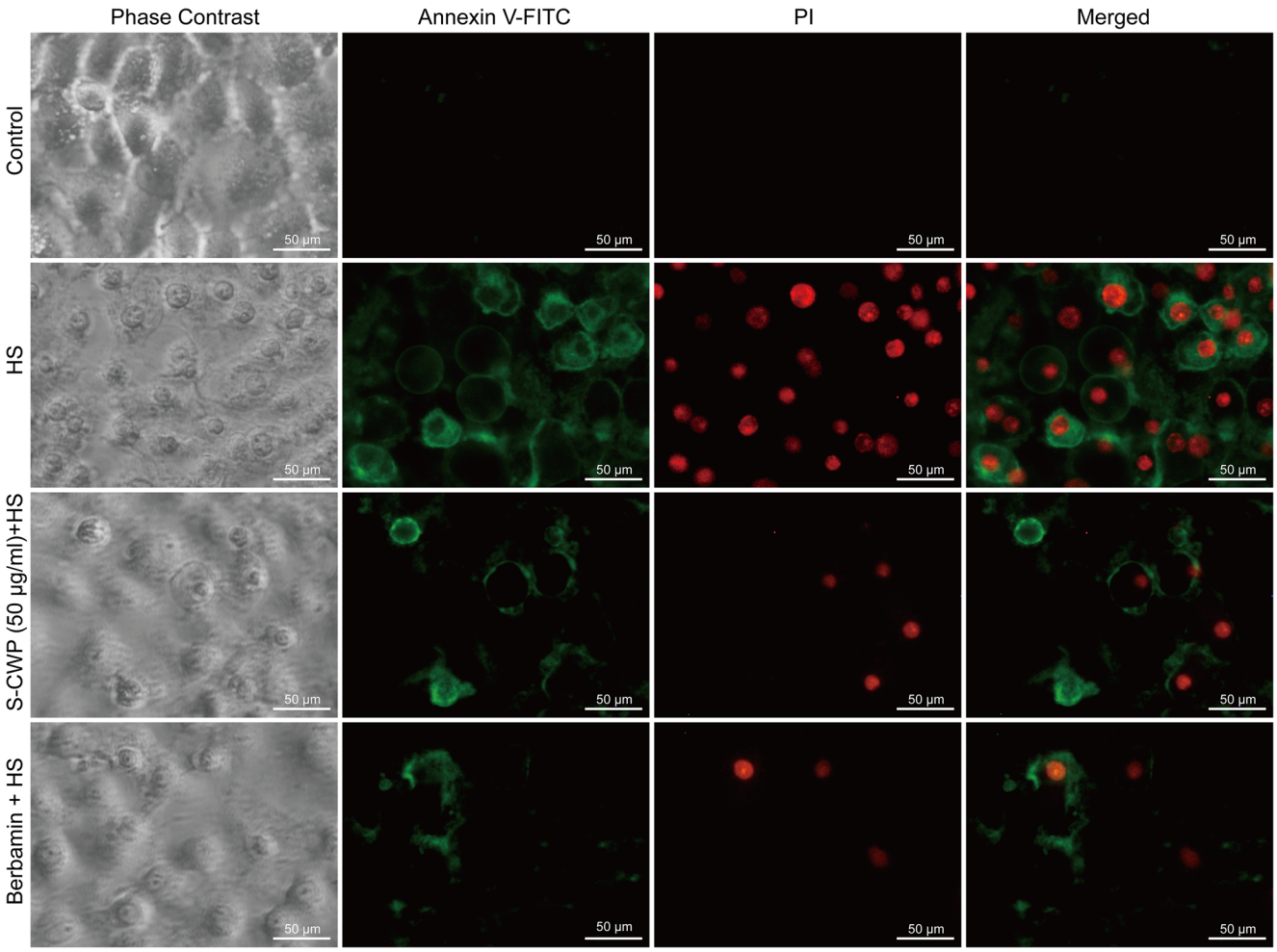


**Fig. 6** S-CWP alleviated HS-induced morphological changes of BRL-3A cells. The green fluorescence in the figure is Annexin V-FITC staining-positive cells (Annexin V-FITC$^+$), and the red is PI staining-positive cells (PI$^+$). Annexin V-FITC$^+$: apoptotic cells. Annexin V-FITC$^+$/ PI$^+$: necrotic and late apoptotic cells. Annexin V-FITC$^-$/ PI$^-$: normal cells. Data are presented as the mean of three determinations ± SEM. $*p < 0.05$, $**p < 0.01$, and $***p < 0.001$

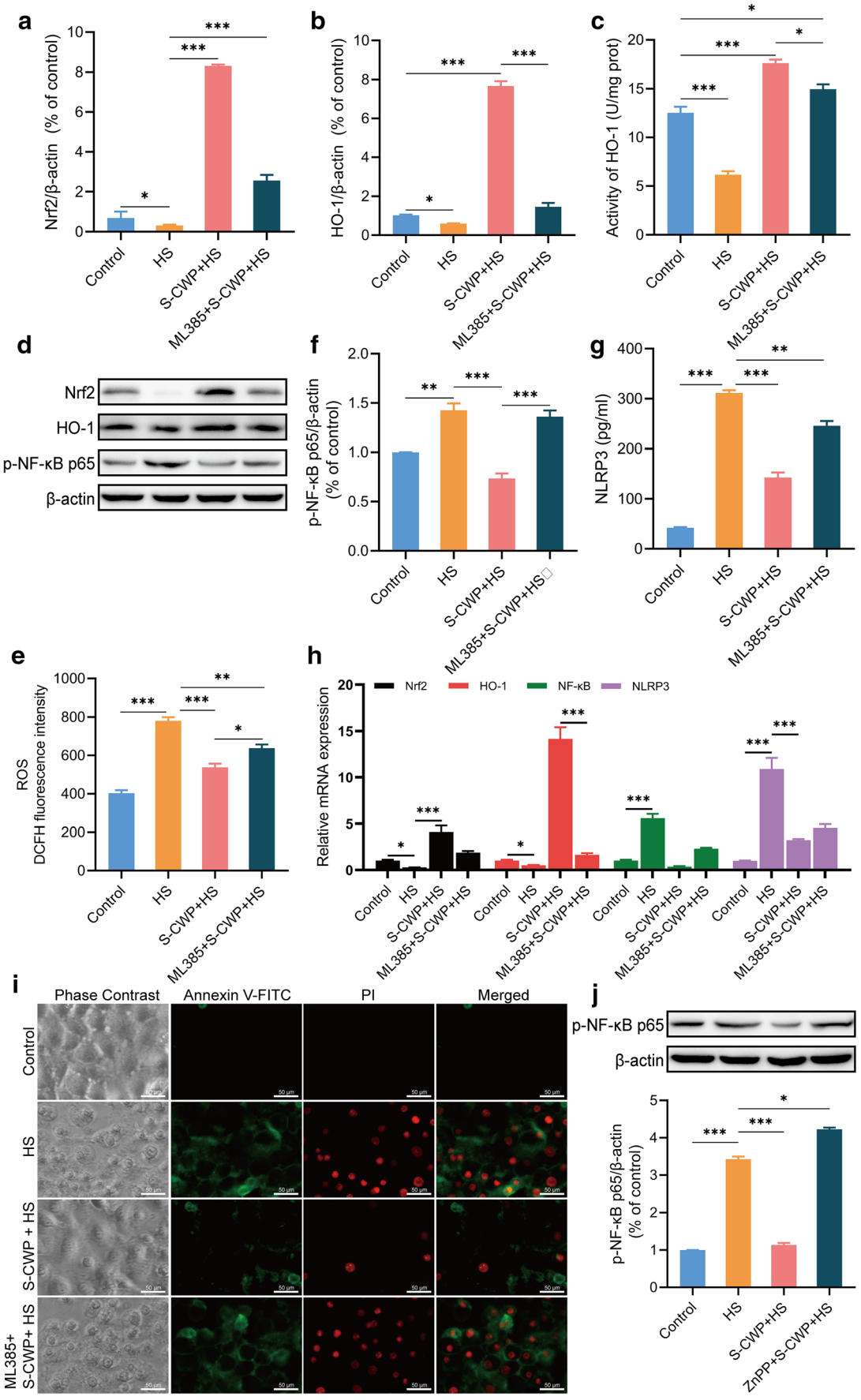
a
Nrf2/β-actin (% of control)
b
HO-1/β-actin (% of control)
c
Activity of HO-1 (U/mg prot)
Control
HS
S-CWP+HS
ML385+S-CWP+HS
d
Nrf2
HO-1
p-NF-κB p65
β-actin
f
p-NF-κB p65/β-actin (% of control)
g
NLRP3 (pg/ml)
e
ROS
DCFH fluorescence intensity
h
Relative mRNA expression
Nrf2
HO-1
NF-κB
NLRP3
i
Phase Contrast
Annexin V-FITC
PI
Merged
Control
HS
S-CWP + HS
ML385+ S-CWP+ HS
j
p-NF-κB p65
β-actin
p-NF-κB p65/β-actin (% of control)
ZnPP+S-CWP+HS

enzymolysis exhibited significantly radical-scavenging activities (Ibrahim et al. 2018), and they are likely to survive transit through the gastrointestinal tract to the target organ (Corrochano et al. 2019). Another study exhibited enhanced antioxidant effects in human endothelial cells pretreated with hydrolyzed WP (O'Keeffe and FitzGerald 2014). In the current study, we provided further evidence that peptides produced by simulated gastrointestinal digestion of CWP (S-CWP) could have beneficial effects on HS-induced rat liver BRL-3A cells damage via the Nrf2/HO-1/NF-κB/NLRP3 antioxidant, anti-inflammatory, and anti-apoptosis signaling pathway.

Excessive production of ROS in cells is the main culprit leading to oxidative stress, which further leads to cell damage by destroying biological macromolecules such as lipids, proteins, and DNA (Hybertson et al. 2011; Sies et al. 2017). As reported, HS increases ROS production by promoting NADPH depletion, while antioxidants protect cells against HS by enhancing the level of NADPH (Lord-Fontaine and Averill-Bates 2002). Oxidative stress further leads to hepatocytic damage and liver dysfunction (Xu et al. 2018). Increased levels of lipid peroxidation products (LPO), protein carbonyls (PCO, A marker of protein damage), and 8-OHdG (A marker of DNA damage) in cells have been recognized as an index of oxidative stress. TBARS, which includes malondialdehyde (MDA) and 4-hydroxynonenal (HNE), is a product of the lipid peroxidation of polyunsaturated fatty acids and has been recognized as an indicator for assessing oxidative stress levels (Mihic et al. 2016). In addition, studies have exhibited that NO is a free radical with high activity, which can react with ROS to produce peroxynitrite ($ONOO^-$) with strong oxidation and then destroy functional tissues (Reed 2011). Glutathione includes both reduced glutathione (GSH) and oxidized glutathione (GSSG). GSH plays an important role in maintaining the appropriate redox states of protein sulfhydryl groups and is a key antioxidant in cells. SOD, CAT, GSH-Px, and HO-1 are the major antioxidant enzymes for controlling ROS levels, and kinds of stress factors impair their functions (Corrochano et al. 2018). In this research, HS remarkably increased the levels of ROS, TBARS, 8-OHdG, PCO, and NO, increased the activity of NADPH oxidase, and decreased the activities of SOD, CAT, GSH-Px, and HO-1, the content of GSH, and the viability of cells. Pretreatment with S-CWP significantly reduced the levels of ROS, TBARS, 8-OHdG, PCO, and NO and NADPH oxidase activity of BRL-3A cells but increased SOD, CAT, GSH-Px, and HO-1 activities and the content of GSH, as well as the cell viability. In particular, S-CWP showed an enhancement to the activity of HO-1, which is an important regulator that protects the cell against oxidative stress. These results indicated that S-CWP could alleviate HS-induced oxidative damage by enhancing the antioxidant capacity of BRL-3A cells.

Except for oxidative stress, HS-induced excess ROS can activate various stress signaling, including NF-κB, which promotes the expression of the NLRP3 inflammasome and causing liver damage in rats (Song et al. 2018). Evidence showed that the NLRP3 inflammasome exhibits a significant role in stress signal-induced liver damage (Szabo and Csak, 2012; Yan et al. 2012). Inflammasomes distribute in both parenchymal and non-parenchymal cells of the liver and are responsible for the activation of caspase-1, which causes pyroptosis. A previous study has shown that HS activated NLRP3 inflammasome in the rat liver, showing increased cappase-1 activity. Activated NLRP3 inflammasome then induced IL-1β activation and hepatocyte pyroptosis, which further aggravates liver damage (Geng et al. 2015). Here, HS upregulated the phosphorylation of NF-κB p65 and the expression of NLRP3 and caspase-1, exhibiting an inflammatory response. In addition, the present study suggested that berbamine dihydrochloride, an inhibitor of NF-κB, down-regulated the expression of P-NF-κB p65, NLRP3, and caspase-3 and alleviated apoptosis. Therefore, we provided additional evidence that S-CWP inhibited the phosphorylation of NF-κB p65 and the levels of NLRP3 and caspase-1, exhibiting an anti-inflammatory activity in BRL-3A cells. Similarly, CWP down-regulated the levels of TNF-α, IL-6, and IL-1β in lymphocytes of HS mice by inhibiting the activation of NF-κB (Badr et al. 2018b). Given the role of ROS in activating NF-κB/NLRP3 inflammasome axis and thus mediating HS-induced liver damage, it could be indicated that this signaling pathway plays an important role in the anti-inflammatory effect of S-CWP.

Accumulating evidence indicates that oxidative stress and inflammation play an important role in mediating HS-induced apoptosis (Badr et al. 2018a, b; Geng et al. 2015; Ramadan et al. 2018; Slimen et al. 2014). There are two main apoptotic pathways, death receptor pathway and mitochondrial pathway (Ramadan et al. 2018). The death receptor pathway is a process of apoptosis mediated by transmembrane receptors, such as the tumor necrosis factor receptor (TNFR) superfamily. The caspase cascade is activated after the receptors combined with their specific ligands (MATSUDA-MINEHATA et al. 2007). During the mitochondrial pathway, excessive ROS leads to increased mitochondrial membrane permeability, followed by the escape of cytochrome C to the cytoplasm and binds to the apoptotic protease activating factor-1 (Apaf-1), thereby initiating caspase cascade and leading to activation of caspase-3 and subsequently apoptosis (Gillies and Kuwana 2014). Caspase-3 participates in both the mitochondrial and the death receptor apoptotic pathways, and it is the final executioner of apoptosis (Sudo and Minami 2010). In the present study, HS-induced oxidative injury and inflammatory response accompanied by activated caspase-3. HS-induced apoptosis was confirmed by morphological observation of apoptotic cells. In addition, we confirmed that HS-induced hepatocyte

apoptosis could be alleviated by inhibiting NF-κB-mediated inflammatory response. Therefore, inhibition of overproduction of ROS and inflammatory response induced by HS can protect cells from apoptosis. S-CWP alleviated apoptosis in HS-administered BRL-3A cells by inhibited activity of caspase-3, which may be attributed to its dual effects to attenuate oxidative stress and inflammation. Similarly, previous studies have shown that CWP alleviated HS-induced apoptosis in mouse lymphocytes and testicular cells (Badr et al. 2017b, 2018a, b). Our findings suggested that targeting oxidative stress and NLRP3 inflammasome with S-CWP may be a therapeutic strategy to alleviate hepatocyte apoptosis after HS.

Hepatocyte damage, including apoptosis, eventually leads to liver dysfunction. In the current study, elevated levels of biomarkers for liver function, including ALT, AST, and ALP, indicate considerable hepatocellular damage. ALT is mainly present in the cytoplasm of hepatocyte, and its elevated levels indicate impaired hepatocyte membrane, increasing membrane permeability. AST is mainly distributed in the cytoplasm and mitochondria of hepatocytes, and its elevated levels indicate damage to these organelles. AST is an indicator of hepatocellular necrosis. ALP is mainly involved in hepatocyte metabolism (Li et al. 2019). Our results showed that S-CWP treatment suppressed ALT, AST, and ALP levels in cell culture supernatant and protected against HS-induced hepatocyte damage. A previous study showed that CM reduced levels of these biomarkers and improved alcohol-induced liver damage (Korish and Arafah 2013). Furthermore, we confirmed that HS upregulated the expression of HSP70 in BRL-3A cells. HSP70 is considered to be the most important and highly conserved member of HSPs in mammalian cells. Under physiological conditions, HSP70 is expressed at low levels in cells, and high temperature and various harmful stresses can induce its expression to improve the anti-stress ability of organisms (Badr et al. 2018b). Intracellular HSP70 maintains protein homeostasis and is also a negative regulator of cytokine production (Martine et al. 2019). However, recent studies have found that overexpressed HSP70 can be released from necrotic cells to the extracellular space, which in turn promotes the secretion of proinflammatory cytokines by activating the NF-κB signaling pathway (Asea et al. 2000; Saito et al. 2005). Therefore, it is necessary to maintain the appropriate expression level of HSP70 in cells. Interestingly, our results showed that S-CWP restored HSP70 expression in HS-treated BRL-3A cells. In short, we provided further evidence that CWP, the protein component of CM, and BAPS produced during gastrointestinal digestion have potential anti-HS-induced hepatocyte injury effects.

Nrf2 is a key regulator of the cellular defense system, playing a protective role by mediating the antioxidant response and anti-inflammatory, and the down-regulation of Nrf2 activity has been proved to be closely related to HS-induced apoptosis (Glory and Averill-Bates, 2016). Under stress conditions, Nrf2 is activated to reduce ROS levels, inflammation, and apoptosis by regulating the expression of a group of cellular protective enzymes, including HO-1, thus preventing oxidative and inflammatory damage (Xu et al. 2018). Here, HS down-regulated the expression of Nrf2, as evidenced by the decreased expression of HO-1 and other antioxidant enzyme activities. In this study, when Nrf2 activity was inhibited by ML385, intracellular ROS production increased, HO-1 expression and activity decreased, and NF-κB phosphorylation level increased, along with increased NLRP3 expression and increased apoptosis. The results indicate that Nrf2 activity is essential for hepatocytes to resist HS-induced damage. Interestingly, S-CWP alleviated HS-induced oxidative stress, inflammatory response, and apoptosis, restored cell viability, and showed its potential regulatory effect on Nrf2 signaling.

Subsequently, we further confirmed that S-CWP significantly upregulated the expression of Nrf2 and HO-1 and the activity of HO-1. The upregulated Nrf2 signaling pathway by S-CWP resulted in increased antioxidants and reduced ROS production and apoptosis. However, the inhibitory effect of S-CWP on NF-κB, NLRP3, and apoptosis was weakened when Nrf2 activity was inhibited by using ML385. Other studies have shown that activation of Nrf2/HO-1 can directly suppress the NF-κB signaling pathway and proinflammatory cytokines (Wardyn et al. 2015). Therefore, our results revealed that S-CWP inhibited NF-κB/NLRP3 inflammasome axis-mediated hepatocyte apoptosis by activating the Nrf2 signaling pathway. Given the obvious enhancement of HO-1 by Nrf2 signaling, we speculated that HO-1 played a major role in the protective effect of S-CWP on HS-induced hepatocyte damage. To investigate the anti-inflammatory effects of the Nrf2/HO-1 axis, a specific inhibitor of HO-1, ZnPP, was used in the present study. Here, we revealed that S-CWP treatment significantly increased the expression of HO-1 and diminished the phosphorylation of NF-κB p65 in HS-treated BRL-3A cells, while these effects blocked in the presence of ZnPP. These results indicated that the upregulated HO-1 in BRL-3A cells contributed to the S-CWP-induced alleviative effects against HS-induced inflammatory reaction and subsequent cell damage.

## Conclusion

In conclusion, our findings demonstrated that S-CWP alleviated HS-induced damage in BRL-3A cells. S-CWP suppressed oxidative stress, enhanced the ability of the antioxidant defense, restored protein homeostatic, and alleviated subsequently inflammatory response and apoptosis in hepatocytes via the Nrf2/HO-1/NF-κB/NLRP3 signaling pathway and hence exhibited a potential protective benefit against HS-induced hepatocyte apoptosis. Additionally, the reported

therapeutic properties of CWP in different pathological conditions make it particularly fascinating. However, the exact molecular mechanism of S-CWP protecting hepatocytes from HS-induced damage is worth further exploration in future studies, and the bioactive peptides in S-CWP also need further identification.

**Acknowledgments** The authors gratefully acknowledge the fund supports. I would like to show my deepest gratitude to Dr. Chunyu Liu for his great help in cell culture.

**Authors' contributions** Donghua Du, Wenting Lv, and Surong Hasi conceived and designed the study; Donghua Du, Rina Su, and Chunwei Yu carried out the investigation; Xiaoxia Jing and Nuwenqimuge Bai contributed analysis data; Donghua Du and Chunwei Yu analyzed the data and drafted the manuscript; and Surong Hasi edited the manuscript. All authors read and approved the final manuscript.

**Funding** This research was funded by the National Natural Science Foundation of China (32060815) and Natural Science Foundation of Inner Mongolia (2020MS03011).

## Compliance with ethical standards

**Conflict of interest** The authors declare that they have no conflict of interest.

## References

Abdel-Aziem SH, Hassan AM, Abdel-Wahhab MA (2011) Dietary supplementation with whey protein and ginseng extract counteracts oxidative stress and DNA damage in rats fed an aflatoxin-contaminated diet. Mutat Res 723:65–71. https://doi.org/10.1016/j.mrgentox.2011.04.007

Abraham NG, Lutton JD, Levere RD (1985) Heme metabolism and erythropoiesis in abnormal iron states: role of delta-aminolevulinic acid synthase and heme oxygenase. Exp Hematol 13:838–843

Akbarian A, Michiels J, Degroote J, Majdeddin M, Golian A, De Smet S (2016) Association between heat stress and oxidative stress in poultry; mitochondrial dysfunction and dietary interventions with phytochemicals. J Anim Sci Biotechnol 7:37. https://doi.org/10.1186/s40104-016-0097-5

Altan O, Pabuccuoglu A, Altan A, Konyalioglu S, Bayraktar H (2003) Effect of heat stress on oxidative stress, lipid peroxidation and some stress parameters in broilers. Br Poult Sci 44:545–550. https://doi.org/10.1080/00071660310001618334

Andersen HR, Nielsen JB, Nielsen F, Grandjean P (1997) Antioxidative enzyme activities in human erythrocytes. Clin Chem 43:562–568

Asea A, Kraeft SK, Kurt-Jones EA, Stevenson MA, Chen LB, Finberg RW, Koo GC, Calderwood SK (2000) HSP70 stimulates cytokine production through a CD14-dependant pathway, demonstrating its dual role as a chaperone and cytokine. Nat Med 6:435–442

Asea A et al (2002) Novel signal transduction pathway utilized by extracellular HSP70: role of toll-like receptor (TLR) 2 and TLR4. J Biol Chem 277:15028–15034. https://doi.org/10.1074/jbc.M200497200

Badr G, Ramadan NK, Sayed LH, Badr BM, Selamoglu Z (2017a) Why whey? Camel whey protein as a new dietary approach to the management of free radicals and for the treatment of different health disorders. Iran J Basic Med Sci 20:338–349

Badr G, Sayed LH, Omar HEM, Abd El-Rahim AM, Ahmed EA, Mahmoud MH (2017b) Camel whey protein protects B and T cells from apoptosis by suppressing activating transcription Factor-3 (ATF-3)-mediated oxidative stress and enhancing phosphorylation of AKT and IkappaB-alpha in type I diabetic mice. Cell Physiol Biochem 41:41–54. https://doi.org/10.1159/000455935

Badr G, Abdel-Tawab HS, Ramadan NK, Ahmed SF, Mahmoud MH (2018a) Protective effects of camel whey protein against scrotal heat-mediated damage and infertility in the mouse testis through YAP/Nrf2 and PPAR-gamma signaling pathways. Mol Reprod Dev 85:505–518. https://doi.org/10.1002/mrd.22987

Badr G, Ramadan NK, Abdel-Tawab HS, Ahmed SF, Mahmoud MH (2018b) Camel whey protein protects lymphocytes from apoptosis via the PI3K-AKT, NF-kappaB, ATF-3, and HSP-70 signaling pathways in heat-stressed male mice. Biochem Cell Biol 96:407–416. https://doi.org/10.1139/bcb-2017-0217

Chen HY, Mollstedt O, Tsai MH, Kreider RB (2014) Potential clinical applications of multi-functional milk proteins and peptides in cancer management. Curr Med Chem 21:2424–2437. https://doi.org/10.2174/0929867321666140205135739

Corrochano AR, Buckin V, Kelly PM, Giblin L (2018) Invited review: whey proteins as antioxidants and promoters of cellular antioxidant pathways. J Dairy Sci 101:4747–4761. https://doi.org/10.3168/jds.2017-13618

Corrochano AR et al (2019) Bovine whey peptides transit the intestinal barrier to reduce oxidative stress in muscle cells. Food Chem 288:306–314. https://doi.org/10.1016/j.foodchem.2019.03.009

Elagamy EI (2000) Effect of heat treatment on camel milk proteins with respect to antimicrobial factors: a comparison with cows' and buffalo milk proteins 68:227–232

Geng Y et al (2015) Heatstroke induces liver injury via IL-1beta and HMGB1-induced pyroptosis. J Hepatol 63:622–633. https://doi.org/10.1016/j.jhep.2015.04.010

Gillies LA, Kuwana T (2014) Apoptosis regulation at the mitochondrial outer membrane. J Cell Biochem 115:632–640

Glory A, Averill-Bates DA (2016) The antioxidant transcription factor Nrf2 contributes to the protective effect of mild thermotolerance (40°C) against heat shock-induced apoptosis. Free Radic Biol Med 99:485–497. https://doi.org/10.1016/j.freeradbiomed.2016.08.032

Guo H, Callaway JB, Ting JP (2015) Inflammasomes: mechanism of action, role in disease, and therapeutics. Nat Med 21:677–687. https://doi.org/10.1038/nm.3893

Hamed H, Gargouri M, Boulila S, Chaari F, Ghrab F, Kallel R, Ghannoudi Z, Boudawara T, Chaabouni S, Feki AE, Gargouri A (2018) Fermented camel milk prevents carbon tetrachloride induced acute injury in kidney of mice. J Dairy Res 85:251–256. https://doi.org/10.1017/S0022029918000250

Hassanein T, Razack A, Gavaler JS, Van Thiel DH (1992) Heatstroke: its clinical and pathological presentation, with particular attention to the liver. Am J Gastroenterol 87:1382–1389

Hybertson BM, Gao B, Bose SK, McCord JM (2011) Oxidative stress in health and disease: the therapeutic potential of Nrf2 activation. Mol Asp Med 32:234–246. https://doi.org/10.1016/j.mam.2011.10.006

Ibrahim HR, Isono H, Miyata T (2018) Potential antioxidant bioactive peptides from camel milk proteins. Anim Nutr (Zhongguo xu mu shou yi xue hui) 4:273–280. https://doi.org/10.1016/j.aninu.2018.05.004

Korish AA, Arafah MM (2013) Camel milk ameliorates steatohepatitis, insulin resistance and lipid peroxidation in experimental non-alcoholic fatty liver disease. BMC Complement Altern Med 13:264

Li C et al (2019) Screening of the hepatotoxic components in Fructus Gardeniae and their effects on rat liver BRL-3A cells. Molecules 24. https://doi.org/10.3390/molecules24213920

Lord-Fontaine S, Averill-Bates DA (2002) Heat shock inactivates cellular antioxidant defenses against hydrogen peroxide: protection by glucose. Free Radic Biol Med 32:752–765. https://doi.org/10.1016/s0891-5849(02)00769-4

Martine P, Chevriaux A, Derangere V, Apetoh L, Garrido C, Ghiringhelli F, Rebe C (2019) HSP70 is a negative regulator of NLRP3 inflammasome activation. Cell Death Dis 10:256. https://doi.org/10.1038/s41419-019-1491-7

Matsuda-Minehata F, Maeda A, Cheng Y, Sai T, Manabe N (2007) Regulation of granulosa cell apoptosis by death ligand–receptor signaling. Anim Sci J 79:1–10

Mihic T, Rainkie D, Wilby KJ, Pawluk SA (2016) The therapeutic effects of camel milk: a systematic review of animal and human trials. J Evid Based Complement Altern Med 21:NP110–NP126. https://doi.org/10.1177/2156587216658846

Miller-Cushon EK, Dayton AM, Horvath KC, Monteiro APA, Weng X, Tao S (2019) Effects of acute and chronic heat stress on feed sorting behaviour of lactating dairy cows. Animal:1–8. https://doi.org/10.1017/S1751731118003762

Nawab A, Ibtisham F, Li G, Kieser B, Wu J, Liu W, Zhao Y, Nawab Y, Li K, Xiao M, An L (2018) Heat stress in poultry production: mitigation strategies to overcome the future challenges facing the global poultry industry. J Therm Biol 78:131–139. https://doi.org/10.1016/j.jtherbio.2018.08.010

Nielsen PM, Petersen D, Dambmann C (2001) Improved method for determining food protein degree of hydrolysis. J Food Sci 66:642–646

O'Keeffe MB, FitzGerald RJ (2014) Antioxidant effects of enzymatic hydrolysates of whey protein concentrate on cultured human endothelial cells. Int Dairy J 36:128–135. https://doi.org/10.1016/j.idairyj.2014.01.013

Power-Grant O, Bruen C, Brennan L, Giblin L, Jakeman P, FitzGerald RJ (2015) In vitro bioactive properties of intact and enzymatically hydrolysed whey protein: targeting the enteroinsular axis. Food Funct 6:972–980. https://doi.org/10.1039/c4fo00983e

Ramadan NK, Badr G, Abdel-Tawab HS, Ahmed SF, Mahmoud MH (2018) Camel whey protein enhances lymphocyte survival by modulating the expression of survivin, bim/bax, and cytochrome C and restores heat stress-mediated pathological alteration in lymphoid organs. Iran J Basic Med Sci 21:896–904. https://doi.org/10.22038/IJBMS.2018.27584.6729

Reed TT (2011) Lipid peroxidation and neurodegenerative disease. Free Radic Biol Med 51:1302–1319. https://doi.org/10.1016/j.freeradbiomed.2011.06.027

Saito K, Dai Y, Ohtsuka K (2005) Enhanced expression of heat shock proteins in gradually dying cells and their release from necrotically dead cells. Exp Cell Res 310:229–236

Salami M, Moosavi-Movahedi AA, Ehsani MR, Yousefi R, Haertlé T, Chobert JM, Razavi SH, Henrich R, Balalaie S, Ebadi SA, Pourtakdoost S, Niasari-Naslaji A (2010) Improvement of the antimicrobial and antioxidant activities of camel and bovine whey proteins by limited proteolysis. J Agric Food Chem 58:3297–3302. https://doi.org/10.1021/jf9033283

Shen H et al (2014) Mouse hepatocyte overexpression of NF-kappaB-inducing kinase (NIK) triggers fatal macrophage-dependent liver injury and fibrosis. Hepatology (Baltimore, Md) 60:2065–2076. https://doi.org/10.1002/hep.27348

Sies H, Berndt C, Jones DP (2017) Oxidative Stress. Annu Rev Biochem 86:715–748. https://doi.org/10.1146/annurev-biochem-061516-045037

Slimen IB, Najar T, Ghram A, Dabbebi H, Ben Mrad M, Abdrabbah M (2014) Reactive oxygen species, heat stress and oxidative-induced mitochondrial damage. A review. Int J Hyperth 30:513–523. https://doi.org/10.3109/02656736.2014.971446

Song J-H, Kim K-J, Chei S, Seo Y-J, Lee K, Lee B-Y (2018) Korean red ginseng and Korean black ginseng extracts, JP5 and BG1, prevent hepatic oxidative stress and inflammation induced by environmental heat stress. J Ginseng Res. https://doi.org/10.1016/j.jgr.2018.12.005

Sudo H, Minami A (2010) Regulation of apoptosis in nucleus pulposus cells by optimized exogenous Bcl-2 overexpression. J Orthop Res Off Publ Orthop Res Soc 28:1608–1613

Szabo G, Csak T (2012) Inflammasomes in liver diseases. J Hepatol 57:642–654. https://doi.org/10.1016/j.jhep.2012.03.035

Udenigwe CC, Aluko RE (2012) Food protein-derived bioactive peptides: production, processing, and potential health benefits. J Food Sci 77:R11–R24. https://doi.org/10.1111/j.1750-3841.2011.02455.x

Wang R, Han Z, Ji R, Xiao Y, Si R, Guo F, He J, Hai L, Ming L, Yi L (2020) Antibacterial activity of trypsin-hydrolyzed camel and cow whey and their fractions. Animals (Basel) 10:10. https://doi.org/10.3390/ani10020337

Wardyn JD, Ponsford AH, Sanderson CM (2015) Dissecting molecular cross-talk between Nrf2 and NF-κB response pathways. Biochem Soc Trans 43:621–626. https://doi.org/10.1042/bst20150014

Weigand K, Riediger C, Stremmel W, Flechtencher C, Encke J (2007) Are heat stroke and physical exhaustion underestimated causes of acute hepatic failure? World J Gastroenterol 13:306–309. https://doi.org/10.3748/wjg.v13.i2.306

Xu D, Xu M, Jeong S, Qian Y, Wu H, Xia Q, Kong X (2018) The role of Nrf2 in liver disease: novel molecular mechanisms and therapeutic approaches. Front Pharmacol 9:1428. https://doi.org/10.3389/fphar.2018.01428

Yan W et al (2012) High-mobility group box 1 activates caspase-1 and promotes hepatocellular carcinoma invasiveness and metastases. Hepatology (Baltimore, Md) 55:1863–1875. https://doi.org/10.1002/hep.25572

Zaboli G, Huang X, Feng X, Ahn DU (2019) How can heat stress affect chicken meat quality? - a review. Poult Sci 98:1551–1556. https://doi.org/10.3382/ps/pey399